Cardiac Positron Emission Tomography:
Overview of Myocardial Perfusion, Myocardial Blood Flow and Coronary Flow Reserve Imaging

Darrell D. Burckhardt, Ph.D.

www.siemens.com/mi

SIEMENS

Table of Contents

Cardiac Positron Emission Tomography: Overview of Myocardial Perfusion, Myocardial Blood Flow and Coronary Flow Reserve Imaging

Introduction

The clinical use of ^{82}Rb and $^{13}NH_3$ cardiac positron emission computed tomography (PET) for semi-quantitative myocardial perfusion imaging (MPI) has increased significantly over the past decade[1,2,3,4,5,6,7,11], due primarily to the increased diagnostic accuracy and prognostic value of PET MPI over stress echocardiography and single photon emission computed tomography (SPECT) in clinical assessment of patients with known or suspected obstructive coronary artery disease (CAD)[3,4]. In efforts to provide objective physiological means of managing patients with CAD, quantitative measures reflecting myocardial blood flow (MBF) and coronary flow reserve (CFR) using dynamic ^{82}Rb and $^{13}NH_3$ PET have likewise received recent attention[4,5,29,30]. Patients with chronic stable CAD, as well as those affected by diffuse and/or balanced multi-vessel disease, often achieve better outcomes when revascularization is deferred and coronary blood flow is improved through intensive pharmacological therapy and lifestyle modification. An automated quantitative analysis of ischemia and stenosis severity utilizing MBF and CFR integrated with routine visual or semi-quantitative MPI can be used objectively to determine whether or not a stenosis requires revascularization thus providing better patient outcomes at lower costs.

Several leading academic institutions have demonstrated, in humans, the feasibility of MBF and CFR achieved with dynamic $^{13}NH_3$ and ^{82}Rb PET[4,5,6,16]. Siemens, in its commitment to continuously develop patient focused, cutting-edge PET technologies, has taken the next step. This paper describes the first* ever, commercially available, comprehensive clinical workflow for the non-invasive, quantitative physiological assessment of CAD and other cardiac disease characterized by angiographically normal coronaries[6].

Unique Imaging Systems for a Unique Imaging Workflow

Proper equipment selection, along with thorough quality assurance is essential to acquire quantitative clinical data for optimizing diagnostic accuracy[8,19,22]. Owing to its widely accepted role in oncology, clinical PET is almost entirely available in a hybrid multi-modality design with computed tomography (CT). Siemens Biograph™ TruePoint™ and mCT (Figure 1), respectively, are leading edge 3-dimensional (3D) lutetium oxyorthosilicate (LSO) high resolution and time-of-flight PET/CT devices capable of simultaneous static, dynamic, and gated cardiovascular imaging through list mode (LM) acquisition[9]. Cardiovascular PET/CT clinical applications can provide assessment of myocardial perfusion, viability, blood flow, coronary flow reserve, neuronal and receptor function, and inflamed and vulnerable plaque as well as state of the art CT angiography (CTA), perfusion and calcium scoring (CAC)[2,10,11]. Integrating the anatomic, hemodynamic, and metabolic characteristics of the interacting effects of coronary artery stenosis and diffuse atherosclerosis with myocardial function and morphology represents a major advance toward comprehensive diagnostic and prognostic workup of CAD[12]. Although, standard cardiac gated stress MPI is the mainstay of cardiovascular imaging[13], an alternative imaging methodology provided by Siemens dynamic PET/CT cardiac workflow (Figure 2) is potentially "game changing." This technique, described in the following sections, allows clinical decisions regarding coronary interventions to be based on additional objective, physiological measures of functional significance of coronary artery stenosis without any complexity, additional radiopharmaceutical administration, or imaging time added to the standard PET/CT MPI examination.

Figure 1. *Siemens Biograph TruePoint (a) and mCT (b) PET/CT devices.*

*Siemens is the only vendor to offer an integrated myocardial blood flow solution (i.e. PET/CT scanner plus FDA-approved software). Of the major PET/CT vendors to date (GE, Philips, Siemens), only Siemens has released an FDA-approved myocardial blood flow solution.

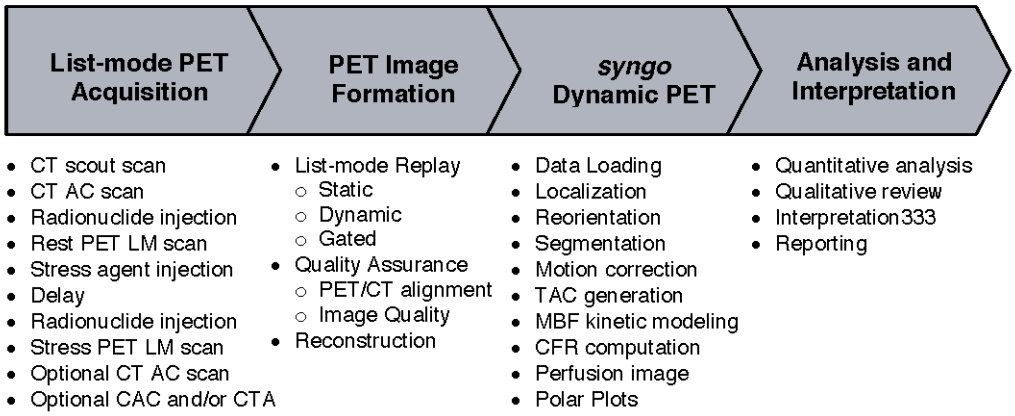

Figure 2. *Dynamic PET/CT cardiac workflow.*

Quality Assurance for Cardiac PET/CT

Quality assurance is imperative to providing optimal clinical results. It is demanding and requires routine maintenance and calibration of the PET/CT and ancillary devices (e.g., infusion pumps, dose calibrators, well counters, gating devices, etc). Clinical PET/CT data must also be inspected routinely for artifacts typically caused by spatio-temporal misalignment resulting from a variety of factors[2,14,15,16,17]. Assuring that early blood pool radioactivity has cleared from the heart is also necessary to avoid adversely affecting PET perfusion image quality and subsequent semi-quantitative MPI polar plots analysis[2,11,16,19,29]. A complete description of quality assurance procedures is beyond this paper's scope and the reader is encouraged to review the American Society of Nuclear Cardiology (ASNC) guideline on the subject[19].

List-mode Acquisition Protocol

Patients are placed head first and supine on the PET/CT patient handling system. An initial low-dose CT scout scan is obtained for proper patient placement in subsequent low-dose CT attenuation correction (CT AC) and PET scans. As stated above, the PET LM imaging protocol does not introduce any additional complexity over standard static or gated MPI acquisitions. Unlike standard ^{82}Rb and $^{13}NH_3$ MPI acquisition start delays of ~90 s and 3 min post-radionuclide administration for blood pool clearance, respectively, dynamic LM acquisition starts with radionuclide administration to obtain data upon radionuclide arrival in the right and left ventricle (LV). The LM acquisition continues for 6-8 min and 10-20 min for ^{82}Rb and $^{13}NH_3$, respectively. Rest and stress arterial radiopharmaceutical administration consist of approximately 1110–1480 MBq (30-50 mCi) ^{82}Rb and 370-740 MBq (10-20 mCi) $^{13}NH_3$ (Table 1). Stress imaging is performed pharmacologically after rest imaging, allowing for radionuclide decay, and the administration of adenosine, dypridamole, or dobutamine. Heart rate, blood pressure and ECG are typically recorded at baseline rest and throughout pharmacological stress imaging. The deliberate generic nature of the protocol described above is meant only to serve as a basis for following sections. Detailed recommendations for cardiac PET imaging procedures, including pharmacologic stress agent and radionuclide administration, are available in the referenced peer reviewed literature [19,20,21,22,23].

During LM acquisition the PET system records incoming timing, event location, and other (phase) information in order of their occurrence (Figure 3).

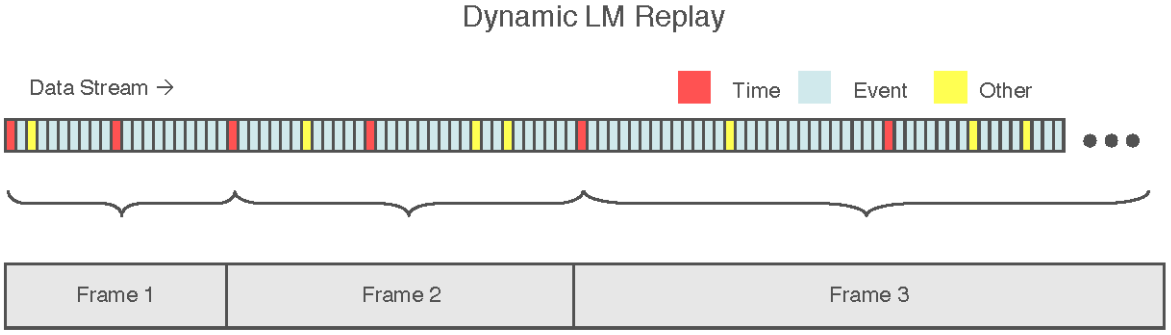

Figure 3. *List-mode data and replay example. The duration of each frame is the same (2 time tags) while the number of events and other tags in the frames are different.*

Dynamic LM PET Image Formation

List-mode (LM) imaging is an ideal approach, in that, multiple image reconstructions (i.e., cardiac and/or respiratory gated, static, dynamic, and summed frames) can be obtained from a single radionuclide administration and LM acquisition. With dynamic LM replay, all data stream events having the same location over a specified time interval or frame are added together and arranged according to projection position and angle to form sinograms. These sinograms are corrected for a variety of physical, geometrical, electronic, and anatomical factors prior to image reconstruction. When properly calibrated, the reconstructed dynamic image sequence represents the continuous time course of radionuclide concentration (Bq/ml) distributed in the blood pool and myocardial tissue regions-of-interest (ROIs), sampled over specific intervals in time as depicted in Figure 4.

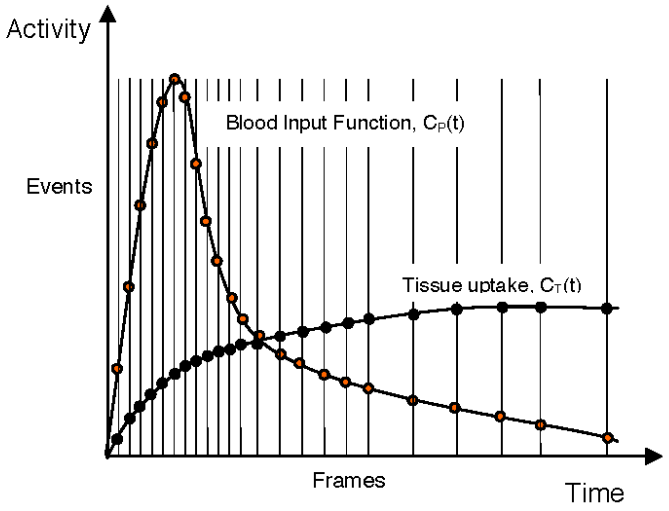

Figure 4. *Time-activity curves. Accumulated events per unit volume over time at an image ROI location are proportional to the radionuclide concentration at the corresponding anatomical location.*

In the preceding example, images are reconstructed for the specific purpose of determining the target tissues radionuclide pharmacodynamics (i.e., blood pool, myocardium time-activity curves). Generally, cardiac and respiratory gated images can be formed using LM replay and other physiological information inserted into the LM data stream obtained from ancillary equipment (e.g., ECG, pressure sensors). While methods for obtaining image derived physiological gating information are reported in the literature[9] they are not currently commercially available and therefore beyond the scope of this paper.

Myocardial Perfusion, Myocardial Blood Flow, and Coronary Flow Reserve

Understanding the basic properties of PET MPI agents is necessary in order to choose the proper agent for a particular clinical setting and to fully understand the results of myocardial perfusion and blood flow imaging [(19)]. Flow imaging agents fall into two basic categories: 1) freely diffusible and 2) soluble substances "trapped" in the myocardium. Usually, only freely diffusible tracers allow for repeated studies due to their rapid physiological washout from the myocardium. H215O is an example of a freely diffusible agent [(24)]. Images of a freely diffusible agent often suffer from poor counting statistics resulting in noisy images of the radionuclide distribution. Soluble agents, however, remain fixed in the myocardium for a sufficient length of time, usually by a metabolic-trapping mechanism, and produce images of reasonable image quality. ^{82}Rb and $^{13}NH_3$ fall into this second category. ^{82}Rb has a short half life (75 s) and therefore quickly disappears from the myocardium allowing rapid repeated imaging studies.

The amount of perfusion agent taken up in a specific area of the myocardium is determined by the tracer's physical properties, delivery (regional coronary blood flow), and myocyte extraction and retention. Both myocyte cell membrane integrity and energy utilization are necessary for intracellular tracer extraction and retention. Thus, retained or "trapped" tracer radioactivity not only indicates the pattern of blood supply but also indicates regional myocyte viability[25]. Accordingly, myocardial regions supplied by "normal" coronary blood flow will possess a "normal" pattern of tracer uptake. Myocardial regions supplied by stenosed coronary arteries will have lower coronary blood flow and reduced uptake relative to normal regional uptake [(26)]. Under resting conditions, however, the reduction in CBF is not always obvious in relative regional uptake even in patients with moderate to severe stenosis (<90%) or with systemic, balanced CAD. However, when myocardial metabolic demand for nutrients and oxygen is increased during exercise or stress conditions, the relative difference between normal and stenotic vascular blood flow is considerable and produces a distinct relative reduction in tracer uptake (i.e., perfusion defect) between normal and ischemic myocardium. This difference in tracer uptake or nonhomogeneity between normal and stenotic vascular territories during stress is the underlying principle establishing myocardial perfusion imaging[27]. Typically, perfusion images, normalized to peak myocardial uptake, are compared to recognized normal population perfusion pattern averages. Normalized perfusion values falling outside their "normal population" regional pattern confidence intervals are quantified as defect extent and severity. For the same region, defects present at stress and absent at rest indicate reversible ischemia while matching rest-stress defects are suggestive of myocardial scarring or infarction. Detection of CAD with MPI, therefore, relies on regional radiotracer uptake differences resulting from stress-induced coronary flow heterogeneity.

	^{82}Rb	$^{13}NH_3$
Administered radioactivity range GBq (mCi) patient < 91 kg (200 lbs) patient < 113 kg (250 lbs) patient > 113 kg (250 lbs)	1.11-1.85 (30-35) 1.11 (30) 1.48 (40) 1.85 (50)	0.37-0.74 (10-20) 0.37 (10) 0.74(20)
Radioactivity infusion/injection maximum rate (ml/min) maximum volume (ml)	 65 50	 12 6
Scan duration (min)	6-8	10-15
Low-dose CT attenuation correction protocol Tube current (effective mAs) Tube voltage (kVp) CTDI vol (mGy) Slice thickness (mm) Scan time (sec)	free-breathing 11 120 0.74 3.0 4	free-breathing 11 120 0.74 3.0 4
Rest-Stress scan separation (min)	10	50
Stress agent rate and period of administration (mg/kg/min → min) Adenosine Dypridamole Dobutamine (see guidelines)	 0.14 → 6 0.14 → 4	 0.16 → 6 0.14 → 4
Radionuclide administration delay post-stress agent administration start (min) Adenosine Dypridamole Dobutamine (≥ 85% age predicted maximum heart rate)	 1.5 3-5	 3 3-5
MPI delay post-radionuclide administration (s)	90 - 120	90 -180
Dynamic frame strategy	12x5s 6x10s 4x20s 4x40s	12x10s 6x30s 2x60s 1x180s
Reconstruction method iterations subsets Zoom (+X direction offset mm) matrix size (pixels) Gaussian filter FWHM (mm)	OSEM 3 8 2.2/2.6 + 30 168x168/128x128 5	2D-OSEM 4 8 2.2/2.6 + 30 168x168/128x128 5

Table 1. *Typical parameters associated with ^{82}Rb and $^{13}NH_3$ dynamic LM studies.*[19,20,21,22,23]

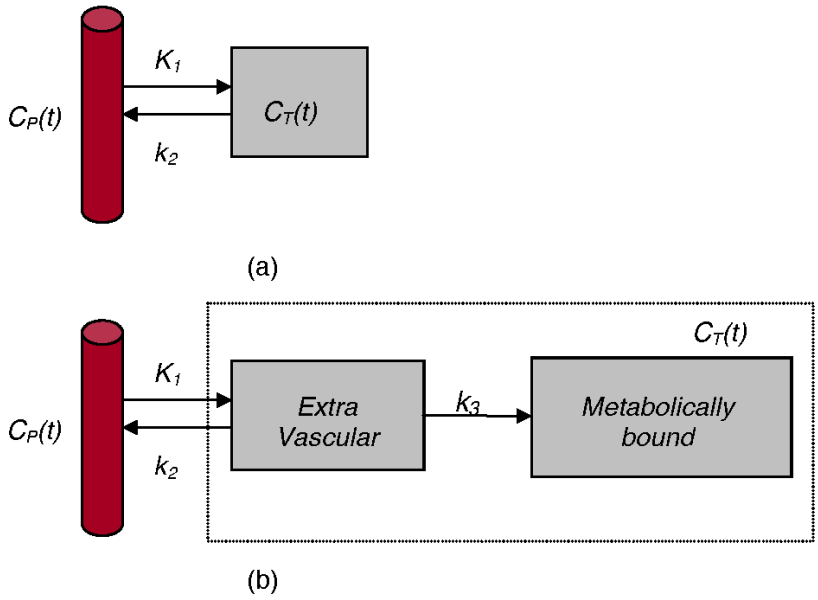

Figure 5. *The one- and two-compartment tracer kinetic models for ^{82}Rb (a) and $^{13}NH_3$ (b), repectively. CP(t) is the blood input function and CT(t) the myocardial tissue compartment. The $^{13}NH_3$ model contains extra-vascular or interstitial "free" and intracellular or "trapped" spaces. K1 represents myocardial extraction, k2 the rate of transport back to the blood, and k3 the rate of $^{13}NH_3$ metabolic conversion into 13N-glutamine.*

The assessment of perfusion tracer uptake patterns, however useful in the identification of normal or ischemic myocardium under stress or exercise conditions, has its limitations. Relative myocardial uptake may appear to be homogeneous ("normal") when myocardial blood flow is abnormal as in patients with balanced coronary blood flow reduction, diffuse or non-occlusive epicardial luminal narrowing of coronary arteries, or an occlusive coronary stenosis in the region with the highest tracer uptake(assumed to have normal blood flow and used as a reference region for normalization). Acute coronary events, majorly, do not originate in coronary arteries with distinct stenosis. The reduction or impairment of blood flow in acute coronary syndrome (ACS) result from plaque rupture, subsequent thrombus formation, and vascular occlusion[28]. Measurements of myocardial blood flow provided by dynamic PET can provide a more objective assessment of the physiological severity and functional consequences of coronary stenosis in the former example and the in the latter example, helps identify patients with pre-clinical arthrosclerosis.

The individual images of a dynamic PET sequence do not necessarily yield clinically relevant information as they are often noisy due to their short duration and image pixels of the myocardium obtained early in the dynamic sequence contain blood pool radioactivity (spill-over). However, tracer kinetic data (TACs) derived from the entire ensemble of early to late dynamic frames can produce a quantitatively accurate estimate of the desired physiological parameter (i.e., regional myocardial blood flow) by a processing procedure called mathematical "tracer kinetic" modeling. The pharmaco-kinetic behavior of ^{82}Rb and $^{13}NH_3$ described by one-[30] and two-tissue compartment mathematical models[31], respectively (Figure 5), are fitted to the discretely sampled patient time-activity curves derived from the dynamic PET series. The model parameters are estimated using non-linear regression by minimizing the differences between the model results and patient time-activity data. The model parameters, which include blood flow, are often constrained to physiologically realistic values, in order to improve the reliability of the parametric model estimates.

Coronary flow reserve (CFR), defined as the amount of additional coronary blood flow that can be supplied to the heart above baseline, is calculated as the ratio of near-maximal vasodilation to basal (stress to rest) MBF. CFR is a measure of both the larger epicardial coronary vessels and the microcirculation[29]. There is a rich amount of literature and excitement on the PET computation of myocardial blood flow and coronary reserve. Impaired flow reserve, in some situations such as, early stage atherosclerosis, is thought to relate to dysfunction of the endothelial control of the microvasculature. Coronary flow reserve, thus, is important not only in evaluating individual coronary stenosis but also the evaluation of a number of disease processes which affect the heart.

Coronary flow reserve can be measured invasively at the time of coronary catheterization. PET, however, has the advantage of making this measurement non-invasively. Siemens seamlessly integrates the compartment kinetic analysis of PET data, without complexity, into the clinical workflow using state-of-the-art PET/CT scanners, acquisition modes, reconstruction methods, and kinetic analysis for quantitative MBF and CFR quantification and review.

Processing of dynamic PET data to obtain MBF and CFR

A number of image processing steps are required to obtain the blood input function and tissue uptake time activities curves for the compartmental tracer kinetic analysis in the determination of MBF and CFR. These steps, described below in the context of their *syngo* implementation, start with the selection of stress and rest dynamic PET (transaxial) image sequences from the *syngo* patient browser followed by loading the data into the MI Circulation application and then launching *syngo* Dynamic PET. Automatically, the weighted sum of the later frames in each dynamic sequence is used to locate delineate, and re-orient the

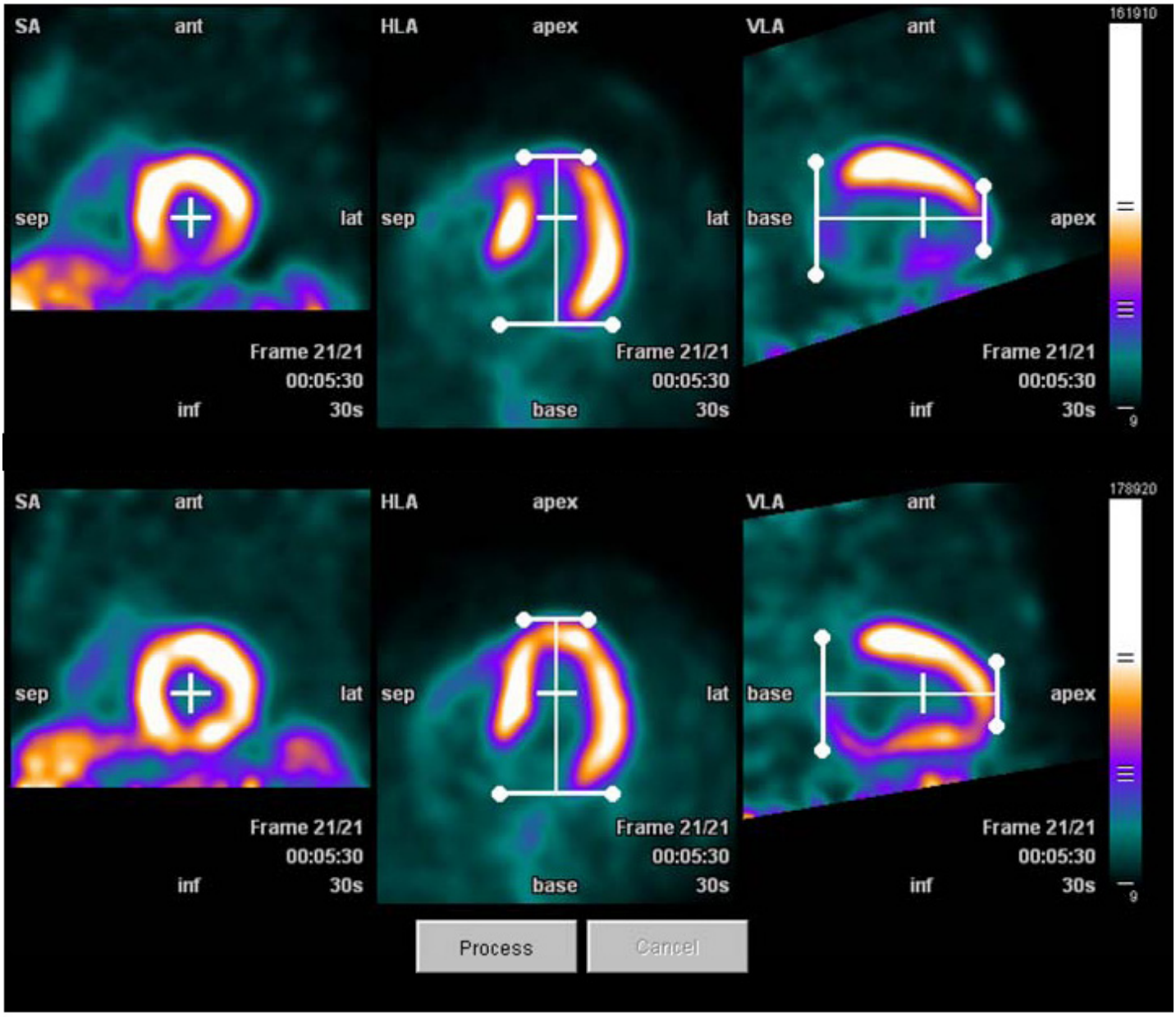

Figure 6. *Automatic heart localization, alignment, and display in standard cardiac orientation.*

LV myocardium along its long-axis for all frames in the dynamic sequence. Stress and rest sequences are stereotactically aligned to each other in standard cardiac orientation. The *syngo* Dynamic PET application also allows for manual adjustments of apex, base and long axis location and angle as needed (Figure 6).

The *syngo* Dynamic PET application uses the conventional cylindrical-spherical model[32] for dynamic myocardial sampling as described below and illustrated in Figure 7. A cylindrical sampling pattern of 36 radial profiles (every 10°) perpendicular to the long-axis is used in each of 9 slices equally spaced over the basal two-thirds of the long-axis. A spherical sampling at 18° intervals in the apical zone is employed, to generate 6 spherical slices. A 10° radial angular sampling angle is also used in the spherical or apical one-third of the myocardium region.

Maximum activity points are obtained along each of the 540 radial profiles of the summed late frame image. Due to the noise in areas of lower myocardial tracer uptake, the location of maximum uptake along the radial profile is not always within the LV myocardium. In this case, special smoothing and interpolation techniques are used to derive the mid-myocardial iso-surface. The mid-myocardial iso-surface is shifted to form endocardial and epicardial boundaries outlining the myocardium (Figure 8). For quality assurance, a persistent overlay of this outline in the three orthogonal views while stepping through the dynamic frame sequence, allows for the assessment of cardiac movement. If necessary, cardiac motion compensation is applied automatically to later frames.

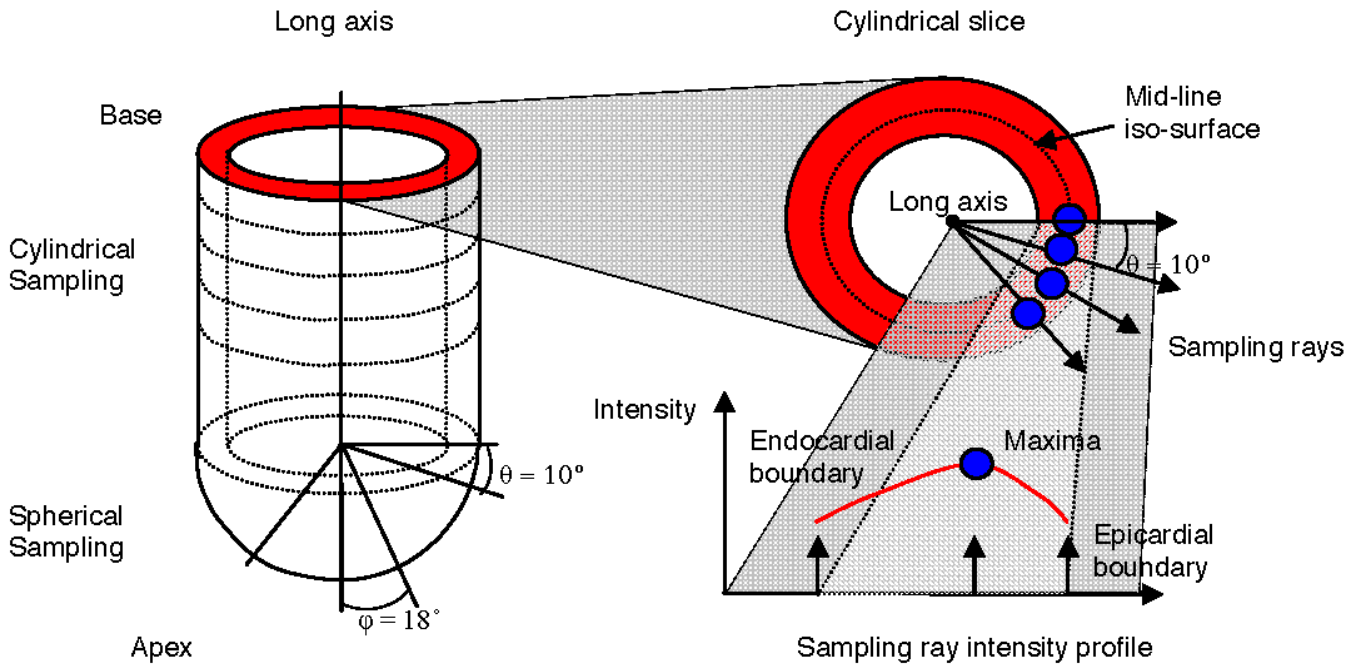

Figure 7. *Left ventricular myocardial sampling strategy.*

Myocardial time-activity curve data points are obtained at each time frame along the radial line segments defined by the epicardial and endocardial boundaries as the averaged value of the neighborhood around the maximum radionuclide concentration. Averaging is performed to reduce the effects of noise, blood partial volume and spill-over effects. The partial volume and spill-over effects are also estimated and accounted for during kinetic modeling. A total of 540 time-activity curves are generated from the myocardium in this fashion.

The blood input function used for all kinetic analyses is obtained from the dynamic sequence by averaging the activity in a cylindrical region-of-interest placed in the middle of the left ventricle in the most basal slice for each time frame. This blood pool ROI is displayed as a green cylindrical overlaid on the three orthogonal views (Figure 8).

Analysis and Interpretation of Clinical Cases

The results of tracer kinetic analysis include polar plots for stress MBF, rest MBF and CFR. For each of the polar plots, an overlay demarking the three main vascular territories from which a parametric chart of the vascular territory statistics (mean and standard deviation) are derived along with a marked out section close to the basal septum is shown Figure 9. For rest and stress, (summed late frame) semi-quantitative MPI polar plots, three orthogonal view displays of dynamic frames, graphed plots of the fitted and actual input function and tissue time-activity curves are also provided. Selecting a segment on any one the polar plots, highlights the same segment in each polar plot and updates the lower left MPI, MBF (QMP) CFR (MPR) values, and the plotted TACs, accordingly.

The screen capture of the *syngo* Dynamic PET application (Figure 9) displays an abnormal patient examination. The data demonstrate the impaired pharmacologic-stimulated myocardial blood flow, resulting in abnormal coronary flow reserve in the LAD and LCX territories and remarkably abnormal CFR in the RCA. The MBF (QMP) for LAD (1.06 ml/g/min) and LCX (1.08 ml/g/min) territories at stress are over twice as high as that of the RCA (0.47 ml/g/min) territory. The rest MBF (QMP) values for the three vascular territories are similar (LAD 0.87, LCX 0.93, RCA 0.7 ml/g/min) with a slightly reduced value for the RCA. The CFR (MPR) values are LAD 1.21, LCX 1.13, and RCA 0.65. The quantitative MBF (QMP) and CFR (MPR) polar plots and values augment as well as correlate well with the concurrent qualitative MPI information, thus demonstrating the potential for a more comprehensive clinical examination and interpretation of the consequences of atherosclerosis on the myocardium and coronary vasculature.

The screen capture of the *syngo* Dynamic PET application (Figure 10) displays an abnormal patient examination. Despite a rather homogenous perfusion distribution at rest, there is a large hypo-perfused fixed apical defect and reduced anterior and lateral wall uptake at stress. The MBF (QMP) for LAD (1.48 ml/g/min) and LCX (1.52 ml/g/min) territories at stress are lower than RCA (2.06 ml/g/min) territory. The rest MBF (QMP) values for the three vascular territories are similar (LAD 1.20, LCX 1.02, RCA 1.25 (ml/g/min)) with slightly reduced value for the LCX. The CFR (MPR) values are LAD 1.24, LCX 1.52, and RCA 1.65. The MBF (QMP) and CFR (MPR) polar plots and quantitative values correlate well with the MPI images and clinical diagnosis.

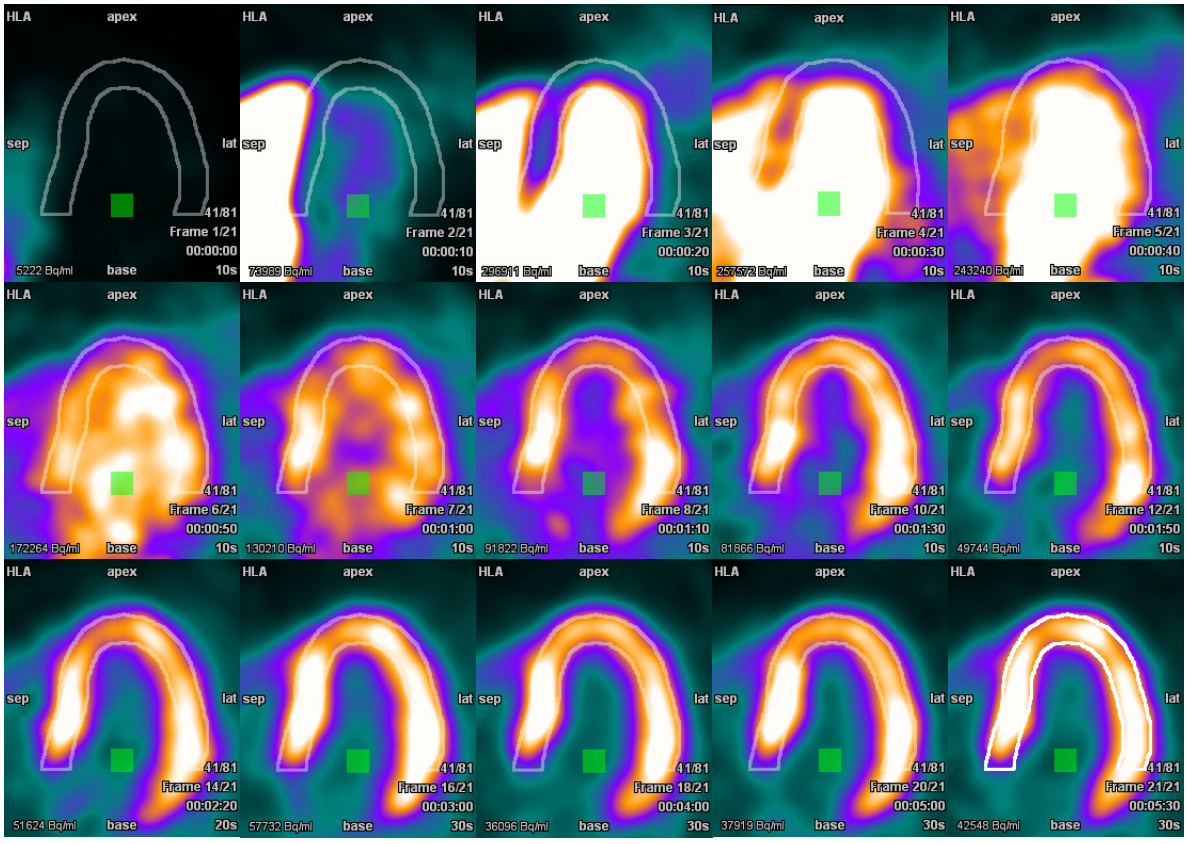

Figure 8. *Segmented myocardial and blood pool regions in dynamic PET frames from which the blood input function and tissue time-activity curves are derived. The radioactivity bolus can be seen entering the right ventricle, the left ventricle, washing out of the blood pool and taken up in the myocardium (upper left then across and down to lower right).*

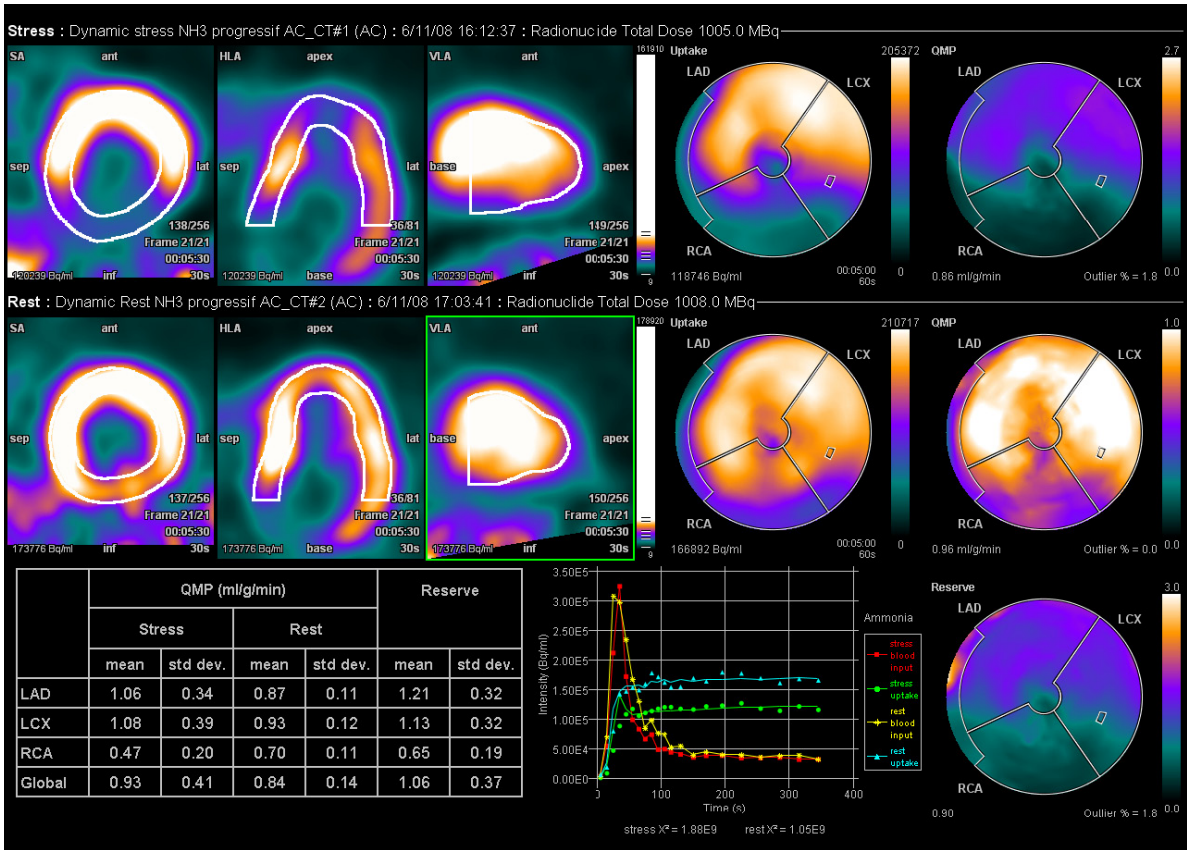

	QMP (ml/g/min)				Reserve	
	Stress		Rest			
	mean	std dev.	mean	std dev.	mean	std dev.
LAD	1.06	0.34	0.87	0.11	1.21	0.32
LCX	1.08	0.39	0.93	0.12	1.13	0.32
RCA	0.47	0.20	0.70	0.11	0.65	0.19
Global	0.93	0.41	0.84	0.14	1.06	0.37

Figure 9. *syngo Dynamic PET display of MBF (QMP) and MPR(CFR) of a $^{13}NH_3$ clinical case showing reversible larger reversible inferio-apical defect.*

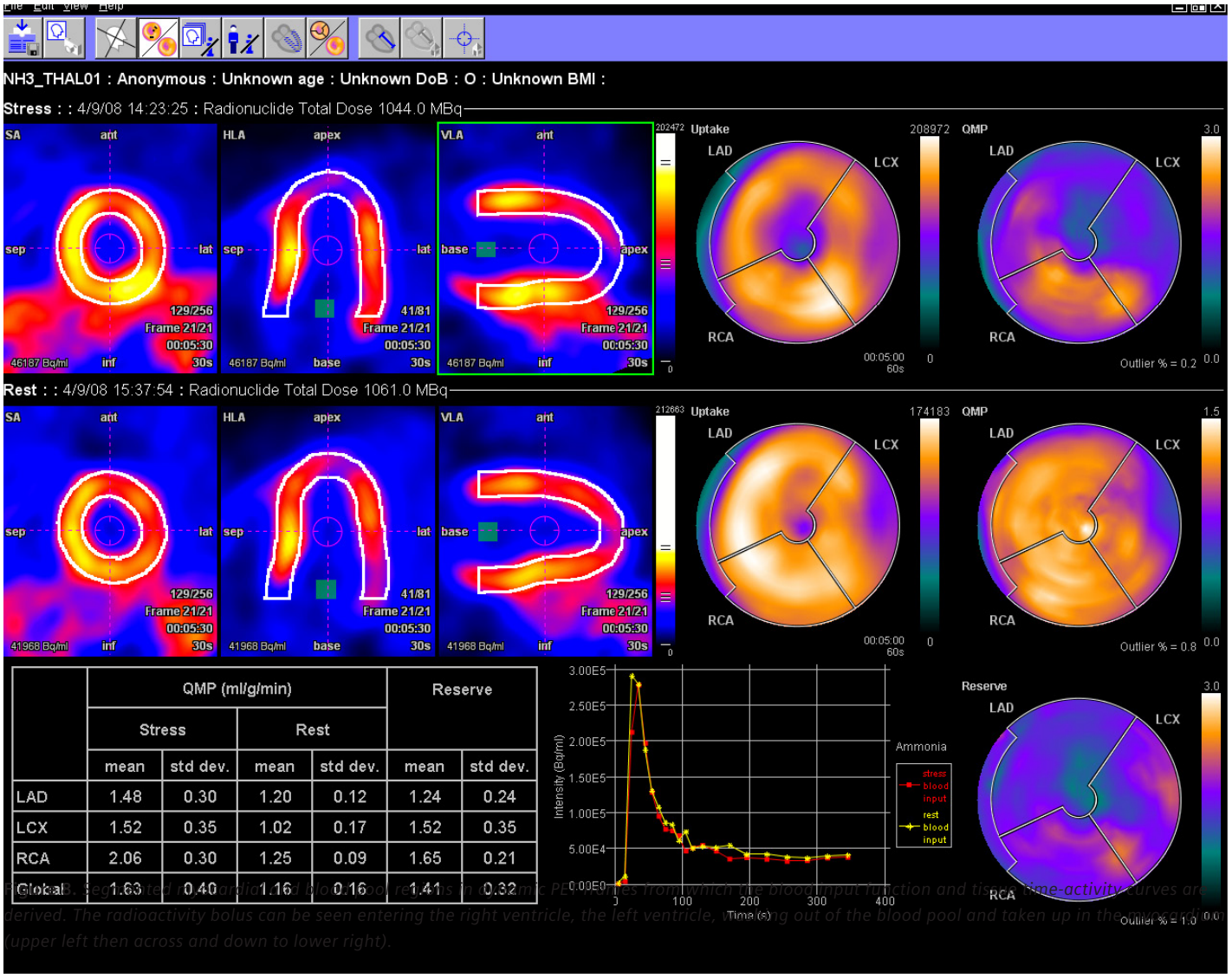

	QMP (ml/g/min)				Reserve	
	Stress		Rest			
	mean	std dev.	mean	std dev.	mean	std dev.
LAD	1.48	0.30	1.20	0.12	1.24	0.24
LCX	1.52	0.35	1.02	0.17	1.52	0.35
RCA	2.06	0.30	1.25	0.09	1.65	0.21
Global	1.63	0.40	1.16	0.16	1.41	0.32

Figure 10. *syngo Dynamic PET display of MBF (QMP) and MPR(CFR) of a $^{13}NH_3$ clinical case showing an apical defect in the stress study.*

Conclusion

The Biograph PET/CT and the *syngo* Dynamic PET application provides for non-invasive assessment of myocardial blood flow and coronary flow reserve with $^{82}Rb^{*}$ and $^{13}NH_3$ using one- and two- tissue compartment tracer kinetic models. The automated technique, provided by Siemens, allows clinical decisions regarding coronary interventions to be based on additional objective, physiological measures of myocardial function without any complexity, additional radiopharmaceutical administration, or imaging time added to the standard PET/CT MPI examination.

Disclaimer

The ultimate judgment about the propriety of any specific procedure or course of action must be made by the physician when considering the circumstances presented.

All that should be expected is that the practitioner will follow a reasonable course of action based on current knowledge, available resources, and the needs of the patient to deliver effective and safe medical care. The sole purpose of this white paper is to assist practitioners in achieving this objective.

** syngo Dynamic PET is FDA-cleared for ammonia and pending validation for rubidium.*

Contributing Authors

Darrell D. Burckhardt, Ph.D. received his graduate degree from The Johns Hopkins University School of Hygiene and Public Health, Department of Environmental Health Sciences, Division of Radiation Health Sciences. Since 1999, Dr. Burckhardt has had a number of responsibilities at Siemens.

Dr. Jérôme Declerck received a Ph.D. in Engineering Sciences from the Institut National de Recherche en Informatique et Automatique (INRIA) and University of Nice (France). He was a visiting scientist at the Johns Hopkins University (Baltimore, USA) in 1998-1999 and has been directing the Science and Technology Team of Siemens Molecular Imaging (formerly Mirada Solutions) since 1999.

Dr. Xiao-Bo Pan received a Ph.D. in flow imaging instrumentation and image analysis from Heriot-Watt University (UK) and a BA in Information and Control Engineering from Xian JiaoTong University (China). She was a Research Associate at the Department of Engineering, University of Oxford, from 1999 and has worked in the Science and Technology Team of Siemens Molecular Imaging (formerly Mirada Solutions) since 2002.

Acronyms and notations

BIF	blood input function
CAD	coronary artery disease
CT	computed tomography
CTA	CT angiography
CFR	coronary flow reserve
FWHM	full width at half maximum
MBF	myocardial blood flow
MPR	myocardial perfusion reserve
$^{13}NH_3$	Nitrogen - 13 radiolabeled ammonia
PET	positron emission tomography
QMP	quantitative myocardial perfusion
^{82}Rb	Rubidium - 82
SPECT	single photon emission computed tomography
TAC	time-activity curve

References

1 ***Kneasurek K, Machac J, Krynyckyi, BR, Almeida OD,*** Comparison of 2-dimensoional and 3-dimensional ^{82}Rb myocardial perfusion PET imaging. *J Nucl Med*. 2003; 44:1350-1356.

2 ***Di Carli MF, Dorball S, Meserve J, El Fakhri G, Sitek A, Moore SC.*** Clinical myocardial perfusion PET/CT. *J Nucl Med* 2007; 48:783-793.

3 ***Sampson UK, Dorbala S, Limaye A, Kwong R, Di Carli MF.*** Diagnostic accuracy of rubidium-82 myocardial perfusion imaging with hybrid positron emission tomography/ computed tomography in the detection of coronary artery disease. *Am Coll Cardiol*, 2*007; 49:1052-1058*.

4 ***Bateman TM, Heller GV, McGhie AI, Friedman JD, Case JA, Bryngelson JR, Hertenstein GK, Moutray KL, Reid K, Cullom SJ.*** Diagnostic accuracy of rest/stress ECG gated Rb-82 myocardial perfusion PET: comparison with ECG-gated Tc-sestamibi SPECT. *J Nucl Cardiol* 2006; 13:24-33.

5 ***El Fakhri G, Kardan a, Sitek A, Dorbala S, Abi-Hatem N, Lahoud Y, Fischman a, Coughlan M, Yasuda T, Di Carli MF.*** Reproducibility and accuracy of quantitative myocardial blood flow assessment with ^{82}Rb PET: Comparison with 13N-ammonia PET. *J Nucl Med* 2009; 50:1062-1071.

6 ***Camici PG, Gropler RJ, Jones T, Abbate AL, Maseri A, Melin JA, Merlet P, Parodi O, Schelbert HR, Schwaiger M, Wijns W.*** The impact of myocardial blood flow quantitation with PET on the understanding of cardiac diseases. *European Heart Journal* 1996; 17:25-34.

7 ***Yoshinaga K, Chow BJW, Williams K, Chen L, deKemp RA, Garrard L, Zeto ALT, Aung M, Davies R, Ruddy TD, Beanlands RSB.*** What is the prognostic value of myocardial perfusion imaging using rubidium-82 positron emission tomography? *J Am Coll Cardiol* 2006; 48:1029-39.

8 ***Nichols KJ, Bacharach S, Bergmann S, Chen J, Cullom SJ, Dorbala S, Ficaro EP, Galt JR, Green Conaway DL, Heller GV, Hyun MC, Links J, Machac J.*** Instrumentation quality assurance and performance. *J Nucl Cardiol* 2007; 14:e61-78.

9 ***Büther F, Dawood M, Stegger L, Wübbeling F, Schäfers M, Schober O, Schäfers KP.*** List Mode – Driven Cardiac and Respiratory Gating in PET. *J Nucl Med* 2009; 50:674–681.

10 ***Wykrzykowska J, Lehman S, Williams G, Parker JA, Palmer MR, Varkey S, Kolodny G, Laham R.*** Imaging of inflamed and vulnerable plaque in coronary arteries with 18F-FDG PET/CT in patients with suppression of myocardial uptake using a low-carbohydrate, high-fat preparation. *J Nucl Med* 2009; 50:563-568.

11 ***Di Carli MF, Hachamovitch R.*** New Technology for Noninvasive Evaluation of Coronary Artery Disease. Circulation 2007;115;1464-1480.

12 **Gould KL.** Physiological severity of coronary artery disease. *Am J Physiol Heart Circ Physiol* 2006 291:2583-2585.

13 **Bengal FM.** Clinical Cardiovascular Molecular Imaging. *J Nucl Med* 2009; 50:837–840.

14 **Nye JA, Esteves F, Votaw J.** Minimizing artifacts resulting from respiratory and cardiac motion by optimization of the transmission san in cardiac PET/CT. *Med. Phys.* 2007; 34:1901-1906.

15 **Martenz-Moller A, Souvatzloglou M, Navab N, Schwaiger M, Nekolla S.** Artifacts from misaligned CT in cardiac perfusion PET/CT studies: frequency, effects and potential solutions. *J Nucl Med* 2007; 48:188-193.

16 **Loghin C, Sdringola S, Gould KL.** Common Artifacts in PET myocardial perfusion images due to attenuation-emission mis-registration: Clinical significance, causes, and solutions. *J Nucl Med* 2004; 45:1029–1039.

17 **Schuster DM, halkar RK, Esteves FP, Garcia, EV, Cook CD, Syed MA, Bowman FD, Votaw JR.** Investigation of emission-transmission misalignment artifacts on rubidium-82 cardiac PET with adenosine pharmacologic stress. *Mol Imaging Biol* 2008; 10:201-208.

18 **Lodge MA, Braess H, Mahmoud F, Suh J, Englar N, Geyser-Stoops S, Jenkins J, Bacharach SL, Dilsizian V.** Developments in nuclear cardiology: Transition from single photon emission computed tomography to positron emission tomography/computed tomography. *J Invasive Cardiol* 2005; 17:491-496.

19 **Dilsizian V, Bacharach SL, Beanlands RS, Bergmann SR, Delbeke D, Gropler RJ, Knuuti J, Schelbert HR, Travin MI.** PET myocardial perfusion and metabolism clinical imaging. *J Nucl Cardiol*. 2009; Jun 4 (Online First).

20 **Strauss HW Miller DD, Wttry MD, Cerqueira MD, Garcia EV, Iskandrian AS, Schelbert HR, Wackers FJ, Balon HR, Lang O, Machac J.** Procedure Guideline for Myocardial Perfusion Imaging 3.3. *J Nucl Med Technol* 2008; 36:155-161.

21 **Henzlova MJ, Cerqueira MD, Hansen CL, Taillefer R, Yao S.** Imaging guidelines for nuclear cardiology procedures: Stress protocols and tracers. *J Nucl Cardiol* 2009; 16. doi: 10.1007/ s12350-009-9062-4.

22 **Hesse B, Tägil K, Cuocolo A, Anagnostopoulos C, Bardiés M, Bax J, Bengel F, Busemann Sokole E, Davies G, Dondi M, Edenbrandt L, Franken P, Kjaer A, Knuuti J, Lassmann M, Ljungberg M, Marcassa C, Marie PY, McKiddie F, O'Connor M, Prvulovich E, Underwood R, van Eck-Smit B; EANM/ESC Group.** EANM/ESC procedural guidelines for myocardial perfusion imaging in nuclear cardiology. *Eur J Nucl Med Mol Imaging*. 2005;32:855–897.

22 **Bokhari S, Ficaro EP, McCallister BD.** Adenosine stress protocols for myocardial perfusion imaging. J Nucl Cardiol 2007; 14:415-6.

24 **Iida H, Kanno I, takahashi A, Miura S, Murakami M, Takahashi K, Ono Y, Shishido F, Inuganmi A, Tomura N.** Measurement of absolute myocardial bolld flow with H215O and dynamic positron-emission tomography. Strategy for quantification in relation to the partial volume effect. Circulation 1988; 78:104-115.

25 **Bhola R, Quaife RA. (2001).** Nuclear cardiology, magnetic resonance imaging and computed tomography. In: Adair OV (Ed.), Cardiology secrets. (2nd ed. pp. 55-65). Philadelphia, PA: Elsevier Health Sciences.

26 **Di Carli MF, Czernin J, Hoh CK, Gerbaudo VH, Brunken RC, Huang , Phelps, and ME, Schelbert HR.** Relation among stenosis severity, myocardial blood flow, and flow reserve in patients with coronary artery disease. Circulation 1995; 91:1944-51.

27 **Jadvar H, Parker JA. (2005).** Chapter 3: Cardiology. In: Parker JA (Ed) Clinical PET and PET/CT. (pp.69-83) New York, NY: Springer.

28 **Vesely MR, Dilsizian V.** Nuclear cardiac stress testing in the era of molecular medicine. *J Nucl Med* 2008; 49:399-413.

29 **Kaufmann PA, Camici PG.** Myocardial blood flow measurement by PET: Technical aspects and clinical applications. *J Nucl Med* 2005; 46:75-88.

30 **Lortie M, Beanlands RS, Yoshinaga K, Klein R, Dasilva JN, DeKemp RA.** Quantification of myocardial blood flow with ^{82}Rb dynamic PET imaging. *Eur J Nucl Med Mol Imaging* 2007; 34:1765-1774.

31 **Hutchins GD, Schwaiger M, Rosenspire KC, Krivokapich, Schelbert H, Kuhl DE.** Non-invasive quantification of regional blood flow in human heart using N-13 ammonia and dynamic positron emission tomographic imaging. *J Am Coll Cardiol* 1990; 15:1032-1042.

32 **Nekolla SG, Miethaner C, Nguyen N, Zegler SI, Schwaiger M.** Reproducibility of a polar map generation and assessment of defect severity and extent assessment in myocardial perfusion imaging using positron emission tomography. *Eur J Nucl Med* 1998; 25:1313-1321.

Some of the radiopharmaceuticals mentioned in this document are not available in all regulatory jurisdictions and/or may not be approved for use for the indications discussed in all countries where they are marketed. Siemens makes no claims of safety or effectiveness and does not endorse any off-label clinical use of radiopharmaceuticals discussed in this paper.

Note: Original images always lose a certain amount of detail when reproduced.

Global Business Unit Address

Siemens Medical Solutions USA, Inc.
Molecular Imaging
2501 N. Barrington Road
Hoffman Estates, IL 60192-2061
USA
Telephone: +1847 304 7700
www.siemens.com/mi

Global Siemens Headquarters

Siemens AG
Wittelsbacherplatz 2
80333 Munich
Germany

Global Siemens Headquarters
Healthcare Headquarters

Siemens AG
Healthcare Sector
Henkestrasse 127
91052 Erlangen
Germany
Telephone: +49 9131 84-0
www.siemens.com/healthcare

Address of legal manufacturer
Siemens Medical Solutions USA
Molecular Imaging
2501 N. Barrington Road
Hoffman Estates, IL 60192-2061
USA

www.siemens.com/mi

Order No. A91MI-10212-1T-7600 | Printed in USA | PA 0909 | © 09.2009, Siemens AG